β-[^{18}F]Fluoro Azomycin Arabinoside (β-[^{18}F]FAZA): Synthesis, radiofluorination and preliminary PET imaging of murine A431 tumors

Piyush Kumar[1], Peter Roselt[2], Gerald Reischl[3], Carlene Cullinane[2], Davood Beiki[4], Walter Ehrlichmann[3], David Binns[2], Ebrahim Naimi[5], Jennifer Yang, Rodney Hicks[2], Hans-Juergen Machulla[3], Leonard I Wiebe

Department of Oncology, Cross Cancer Institute, 11560 University Avenue, Edmonton, Alberta, Canada T6G 1Z2

[2]Peter McCallum Cancer Institute, Melbourne, Australia

[3]Department of Preclinical Imaging and Radiopharmacy, University of Tübingen, Tübingen, Germany.

[4]Current addresses: Research Institute for Nuclear Medicine, Tehran University of Medical Sciences, Tehran 14114, Iran

[5] Current address: Naimi, Ebrahim Pharmacy Ltd., 9452 118 Ave NW, Edmonton, Canada

[1] Correspondence: Piyush Kumar PhD, Department of Oncology, Cross Cancer Institute, 11560 University Avenue, Edmonton, Alberta, Canada T6G 1Z2; E-mail: pkumar@ualberta.ca; Phone: +1(780) 989-4313; Fax: +1(780) 432-8483

Abstract

Background. 1-α-D-(5-Deoxy-5-[^{18}F]fluoroarabinofuranosyl)-2-nitroimidazole ([^{18}F]FAZA) is a PET radiotracer currently used to image regional hypoxia in a wide range of solid tumors in cancer patients. [^{18}F]FAZA is radiofluorinated in moderate recovered radiochemical yield (rRCY) via nucleophilic substitution of the 1-α-D-(2,3-di-*O*-acetyl-5-tosyl)-AZA precursor.

Hypothesis. It is postulated that the β-conformer of FAZA, 1-β-D-(5-fluoro-5-deoxyarabinofuranosyl)-2-nitroimidazole (β-FAZA), by dint of the relative stability of the *C1'* β-anomeric bond to base-catalysed hydrolysis and / or the fidelity of nucleophilic substitution at *C5'*, may offer improved rRCY. Preliminary PET images of the biodistribution of β-[^{18}F]FAZA in a hypoxic tumor-bearing animal model are reported.

Results. The synthesis of β-FAZA and β-[^{18}F]FAZA are now reported. β-FAZA was synthesized by coupling 2-nitroimidazole (AZA) with the appropriately-protected furanose sugar to afford 1-β-D-(2,3-di-*O*-acetylarabinofuranosyl)-2-nitroimidazole (β-Ac_2AZA). Fluorination of β-Ac_2AZA with DAST, followed by alkaline hydrolysis, afforded the title compound in an overall yield of 21%. The radiolabeling synthon, 1-β-D-(5-*O*-toluenesulfonyl-2,3-di-*O*-acetylarabinofuranosyl)-2-nitroimidazole (β-Ac_2TsAZA), was synthesized using reported methods. Radiofluorination of β-Ac_2TsAZA using ^{18}F/K_{222} complex under various reaction conditions afforded β-Ac_2[^{18}F]FAZA in 5 to 51 % radiochemical yield. Deacetylation of this product gave β-[^{18}F]FAZA, which was radiochemically stable for at least 8 h when stored in aqueous ethanol (8%) at 22 °C. Whole body PET imaging with β-[^{18}F]FAZA in A431 tumor-bearing nude mice showed strong uptake in hypoxic regions of the tumor.

Conclusions. β-FAZA and β-Ac_2TsAZA were readily synthesized using standard chemical approaches. Radiofluorination of β-Ac_2TsAZA and the deprotection of β-Ac_2[^{18}F]FAZA were facile, but tended to give rise to a more complex mixture of radiofluorinated by-products than observed when radiolabeling the corresponding precursor of α-[^{18}F]FAZA. Preliminary PET images were indicative of hypoxia-selective accumulation of β-[^{18}F]FAZA. Additional in vitro and in vivo studies are required to demonstrate its potential advantages over [^{18}F]FAZA.

Keywords: hypoxia, PET imaging, β-FAZA, β-[^{18}F]FAZA, FAZA, [^{18}F]FAZA

Introduction

Many solid tumors demonstrate abnormal invasive growth and aberrant vasculature. The resultant oxygen-deficient (hypoxic) tumor microenvironment produces cells that are more resistant to radiation therapy than adjacent, normally oxygenated cells within the tumor.[1,2] Hypoxia gives rise to a myriad of molecular and biological changes that lead to metastatic progression, genetic alterations, recurrence, and ultimately to treatment failure.[3-5] Confirmation of the presence of hypoxic regions in tumors may therefore lead to improvements in individual treatment planning, disease progression monitoring, more accurate prognosis and better therapeutic outcomes.[6,7]

Oxygen-reversible single-electron intracellular bioreduction of nitroimidazoles in hypoxic cells, and the consequent covalent reaction of these reduction intermediates with cellular nucleophiles [8] forms the basis for their selective toxicity to oxygen-deficient tissues.[9] The clinical utility of radiolabeled nitroimidazoles for non-invasive (imaging) diagnosis of focal hypoxia in a variety of pathological disorders is rationalized on these properties.[10] Several ^{18}F-labeled nitroimidazole-based tracers, including 1-α-D-(5-fluoro-5-deoxyarabinofuranosyl)-2-nitroimidazole ([^{18}F]FAZA), are used transglobally to image tumor hypoxia in cancer patients. It is postulated that all azomycin-based hypoxia imaging agents undergo quantitative binding / metabolic trapping to similar degrees, but they produce contrast-variable in vivo images that reflect their unique lipophilicity, diffusion and blood clearance kinetics.[11,12]

The pharmacokinetic attributes of the ideal hypoxia radiotracer include a high volume of distribution based on rapid, ubiquitous perfusion into all tissues, rapid cellular permeation of plasma membranes, rapid clearance from the vascular and non-hypoxic (i.e. non-target) tissue compartments, and rapid redistribution from non-hypoxic depots (i.e., lipoidal tissue) to hypoxic regions. Although [^{18}F]FAZA and other [^{18}F]-labeled azomycin-based hypoxia imaging agents (e.g., [^{18}F]FMISO) (Fig. 1) by and large meet these requirements, their ultimate biodistribution is concentration-diffusion dependent and therefore their accrual maxima in target tissue are constrained by their rapidly falling intravascular concentrations. It has been hypothesized that facilitative or concentrative transporter-assisted, trans-membrane movement of nitroimidazoles by nucleoside [13], peptide [14] or glucose [15-17] transporters could assist in delivering higher concentrations of the nitroimidazole in hypoxic cells.

Radiofluorinated diagnostic radiopharmaceuticals are prepared via several basic approaches, including the most popular nucleophilic substitution using the appropriate synthon.[18] Although nucleophilic substitutions are well understood and easily controlled under many conditions, their application in

radiopharmaceutical syntheses provides unique challenges.[19] For the synthesis of azomycin nucleosides, including FAZA and β-FAZA (Fig. 1), these challenges lie not only in the impact of low reagent concentration, competition by water and quality of the radiofluoride, but on post-radiofluorination competing reactions that are introduced during the deprotection of the labeled product and the unreacted synthon. Competing reactions include elimination of the leaving group at *C5*' concomitantly with elimination of a *C4*' atomic substituent, hereby giving the non-fluorinated *C4'-C5'* alkene counterpart without the desired substitution of the leaving group, or through nucleophilic fluorination at *C5'* and elimination at *C2'-C3'* to form the fluorinated 2'-3' oxirane. Elimination is favored under anhydrous conditions because the nucleophilic fluoride ion also acts as a strong Lewis base under these conditions.[20] Nucleophilic displacement of the nitro group at imidazole *C2* by (radio)fluorine is facilitated by the powerful electron-withdrawing nitro group [21], and although this reaction is better known for 2-nitroimidazoles that have other electron-withdrawing substituents, it has been observed under forcing conditions used to incorporate fluorine for iodine substitutions in azomycin nucleosides.[22] Finally, deprotection following radiofluorination may be incomplete due to conformationally-induced differential sensitivity of the *C2'*- and *C3'* acetyl esters, and is accompanied by a substantial risk for nucleoside decomposition and/or anomerization of the α-*C1'* nucleoside bond to the β-*C1'* anomer [23]

This paper describes the synthesis of β-FAZA and addresses aspects of its radiofluorination chemistry. A preliminary β-[^{18}F]FAZA PET image from a murine tumor model demonstrating its accumulation in hypoxic regions is also provided.

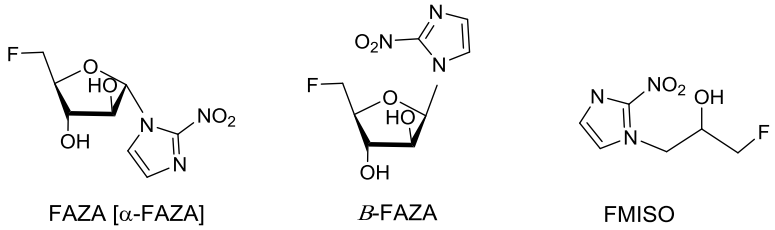

FAZA [α-FAZA] *B*-FAZA FMISO

Figure 1. Chemical structures of α-FAZA, β-FAZA and FMISO

Experimental

Melting points were determined on a Büchi capillary apparatus, and are uncorrected. ^{1}H, ^{13}C and ^{19}F NMR spectra were recorded on a Bruker AM-300 spectrometer in $CDCl_3$ or D_2O; chemical shifts are given in ppm (δ) downfield from tetramethylsilane (^{1}H and ^{13}C) and fluorotrichloromethane (^{19}F) as

internal standards. ^{1}H NMR assignments were confirmed by selective decoupling experiments, and ^{13}C NMR resonances were assigned using the *J* modulation spin echo technique to determine the number of hydrogen atoms attached to each carbon atom. Sugar atoms are identified by a 'prime' (') superscript. Thin layer chromatography (TLC) was performed on Whatman MK6F silica gel micro TLC plates (25 μm thickness) using hexanes:ethyl acetate 1:3, v/v (solvent system A) and hexanes:ethyl acetate 1:1, v/v (solvent system B) as developing solvents. Column chromatography was carried out on Merck 7734 silica gel (100-200 μm particle size). New compounds were characterized by elemental analyses for C, H and N, or by Fast Atom Bombardment (FAB) mass spectrometry using a sodium probe on an AEI-MS-12 mass spectrometer. Acetonitrile (CH_3CN) and Kryptofix2.2.2 (K_{222}) were obtained from Merck (Darmstadt, Germany), and dimethyl sulfoxide (DMSO, dried over molecular sieve) was purchased from Fluka. Sep-Pak light, Accell Plus QMA and Alumina N cartridges were purchased from Waters, USA. Phenomenex Luna pre-column (C18/2, 50 x 10 mm; 5 μm), Phenomenex Nucleosil columns (C18, 250 x 10 mm; 5 μm and C18, 250 x 4.6 mm) and 0.22 μm Millex GS and LX filters were purchased from Millipore, USA.

Synthetic Chemistry

1-β-D-(2,3-Di-*O*-acetylarabinofuranosyl)-2-nitroimidazole (β-Ac_2AZA; **3**; Fig. 2) was prepared either from commercially available 1-β-D-(ribofuranosyl)-2-nitroimidazole **1** by inversion of configuration at *C2'* (six steps) of the furanose ring, or from 1-β-D-(arabinofuranosyl)-2-nitroimidazole **2** (Fig. 2) using selective protection and deprotection of *C5'*-OH as shown in Scheme 1, using reported procedures (m.p. 102-104 °C) [24]. 1-β-D-[5-*O*-Toluenesulfonyl-2,3-di-*O*-acetylarabinofuranosyl]-2-nitroimidazole (β-Ac_2TsAZA; **5**; m.p. 117-119 ºC) was also prepared from **3,** using a literature method.[24]

1-β-D-[5-Fluoro-5-deoxy-2,3-di-*O*-acetylarabinofuranosyl]-2-nitroimidazole (β-Ac_2FAZA; **4**). Diethylaminosulfurtrifluoride (DAST) (51.4 mg; 0.034 mmol) in anhydrous dichloromethane (10 mL) was cooled to -78 ºC. A solution of **3** (105 mg; 0.32 mmol) in anhydrous dichloromethane (10 mL) was added to the DAST solution under stirring and the reaction was allowed to proceed at -78 ºC for 3 h. Additional DAST (0.034 mmol) was added to this reaction mixture after 3 h since the TLC showed that **3** was only partially consumed. The reaction mixture was then allowed to warm to room temperature (22 ºC) and stirred for an additional 16 h. The contents were cooled to 0 °C over ice, unconsumed DAST was quenched with few drops of methanol, and then the solvent was evaporated (rotary evaporator) under water aspirator vacuum. The residue was purified on a silica gel column

using ethyl acetate/hexanes (60/40, v/v) as eluent to afford unreacted **3 (**30 mg) and **4 (**25 mg; 30% yield; m.p. 112-114 °C). ^{1}H NMR ($CDCl_3$): δ 1.85 and 2.17 (two s, each for 3H, 2 X $COCH_3$), 4.27 (d, $J_{3',4'}$=2.8 Hz of d, $J_{5',4'}$=2.6 Hz of d, $J_{5'', 4'}$=3.7 Hz, $J_{F,4'}$=25.9 Hz 1H, *H4'*), 4.71 (d, $J_{4',5''}$=3.7 Hz of d, Jgem=10.7 Hz of d, $J_{F,5''}$=46.0 Hz, 1H, *H5''*), 4.76 (d, $J_{4',5'}$=2.6 Hz of d, Jgem=10.6 Hz of d, $J_{F,5'}$=47.5 Hz, 1H, *H5'*), 5.21 (d, J3',2'=4.6 Hz of d, $J_{4',3'}$=2.8 Hz 1H, *H3'*), 5.73 (d, $J_{3',2'}$=4.6 Hz of d, $J_{1',2'}$=4.3 Hz, 1H, *H2'*), 6.86 (d, $J_{2',1'}$=6.9, 1H, *H1'*), 7.19 (s, 1H, imidazole *H4*), 7.57 (s, 1H, imidazole *H5*); ^{13}C NMR (CD_3OD): δ 19.96 and 20.61 (two s, *C*H_3 of two acetyl groups), 74.61 (*C2'*), 74.86 (d, $J_{F,C}$=6.6 Hz, *C3'*), 80.82 (q, $J_{F,C}$=174.7 Hz, *C5'*), 81.54 (d, $J_{F,C}$=19.8 Hz, *C4'*), 87.41 (*C1'*), 122.98 (d, $J_{F,C}$=3.3 Hz, *C5*), 128.25 (*C4*) and 145.31 (imidazole *C2*), 168.35 and 169.64 (two *C*=O); ^{19}F NMR ($CFCl_3$ as external standard): δ -69.37 (d, $J_{4',F}$=25.9 Hz of d, $J_{5',F}$=47.5 Hz of d, $J_{5'',F}$=45.7 Hz) ppm. CHN analysis for $C_{12}H_{14}FN_3O_6$ (331.25): calc'd. C 43.51; H 4.26, N 12.69; found C 43.56, H 4.11, N 12.32.

1-β-D-[5-Fluoro-5-deoxyarabinofuranosyl]-2-nitroimidazole (β-FAZA; **6**). β-Ac_2FAZA (**4;** 30 mg; 0.091 mmol) was dissolved in a solution of 2M NH_3 in methanol (10 mL) and allowed to stir at 0 ˚C for 1.5 h, after which the solvent was evaporated on a rotary evaporator and the contents chromatographed on a silica gel column using ethyl acetate/hexanes (1:1, v/v) as eluent to afford **6** (15 mg; 70% yield). ^{1}H NMR (CD_3OD) δ 4.00 (m, 1H, *H3'*), 4.07 (m, $J_{3',4'}$=2.8 Hz, $J_{5',4'}$=2.8 Hz, $J_{5'', 4'}$=4.0 Hz, $J_{F,4'}$=24.4 Hz 1H, *H4'*), 4.47 (d, $J_{3',2'}$=5.3 Hz of d, $J_{1',2'}$=5.5 Hz of d, $J_{F,2'}$=1.2 Hz 1H, *H2'*), 4.69 (d, $J_{4',5''}$=4.0 Hz of d, Jgem=10.7 Hz of d, $J_{F,5''}$=48.8 Hz, 1H, *H5''*), 4.76 (d, $J_{4',5'}$=2.8 Hz of d, Jgem=10.7 Hz of d, $J_{F,5'}$=48.8 Hz, 1H, *H5'*), 6.74 (d, $J_{2',1'}$=5.5, 1H, *H1'*), 7.15 (s, 1H, imidazole *H4*), 7.64 (s, 1H, imidazole *H5*); ^{13}C NMR (CD_3OD) δ: 74.55 (d, $J_{F,C}$=6.6 Hz, *C3'*), 77.48 (*C2'*), 82.43 (q, $J_{F,C}$=171.4 Hz, *C5'*), 83.48 (d, $J_{F,C}$=18.7 Hz, *C4'*), 90.47 (*C1'*), 124.19 (d, $J_{F,C}$=5.5 Hz, imidazole *C5*), 128.07 (imidazole *C4*) and 145.31 (imidazole *C2*); ^{19}F NMR ($CFCl_3$ as external standard): δ -65.79 (d, $J_{4',F}$=24.4 Hz of d, $J_{5',F}$=48.8 Hz of d, $J_{5'',F}$=48.8 Hz) ppm; HRMS (ES^+) for $C_8H_{10}N_3O_5FNa$: calc'd, 270.04967; found 270.270.04937 (M^+Na abundance 98.93%).

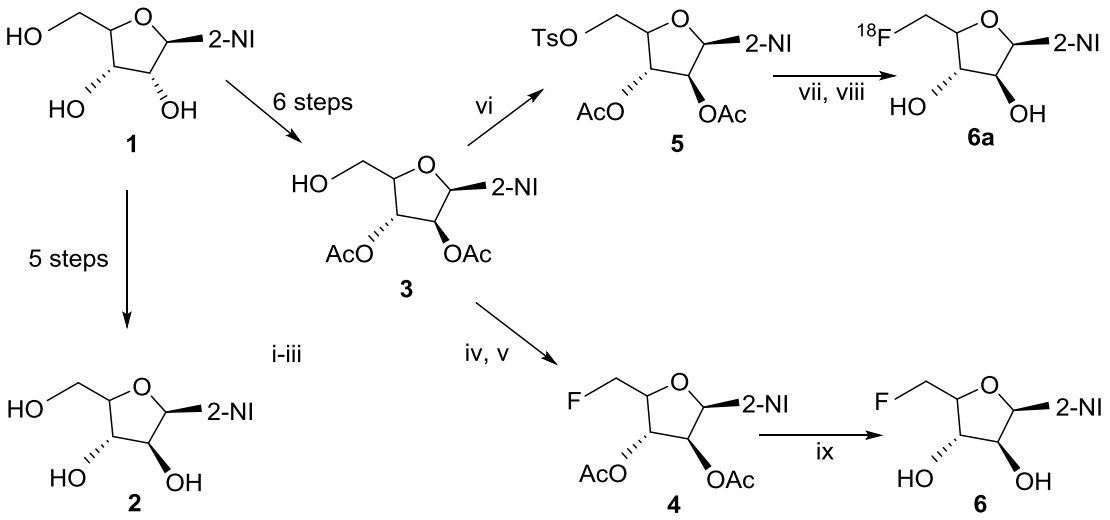

Figure 2. Scheme for the synthesis of β-FAZA and β-[^{18}F]FAZA; reagents and conditions: i) TBDPS-Cl/pyridine, 22 °C, 4 h; ii) Ac_2O/pyridine, 22 °C, 4 h; iii) KF/benzoic acid in CH_3CN, 1 h, 70 °C; iv) DAST, 0-22 °C, 24 h; v) MeOH (a few drops); vi) tosyl chloride/ pyridine, 15 °C, 4 h; vii) K_{222}, K_2CO_3, 5 min, 60 or 80 °C (ASU); ix) 0.1N. NaOH/Dowex H^+ resin.

Radiochemistry

General methods: β-[^{18}F]FAZA was synthesized from **5** in two collaborating centres. [^{18}F]Fluoride was produced via the $^{18}O(p,n)^{18}F$ nuclear reaction on [^{18}O]-enriched (>90%) water using either 12 MeV protons (OSCAR 7 cyclotron, Oxford Instruments, Oxford, UK; Peter MacCallum Cancer Institute, Melbourne, Australia) or 16.5 MeV protons (PETtrace cyclotron, General Electric Healthcare, Uppsala, Sweden; University of Tübingen, Germany). A Coincidence (GE Medical Systems, Milwaukee, WI, USA) FDG automated synthesis unit (ASU) in Melbourne, or a TRACERlab FX_{F-N} ASU (GE Healthcare, Münster, Germany) in Tübingen were used to recover and work-up [^{18}F]fluoride, and to conduct radiofluorinations.

Coincidence ASU method: [^{18}F]Fluoride was adsorbed onto a preconditioned (10 mL aqueous 1N $NaHCO_3$, 10 mL water, 5 mL CH_3CN) ion exchange cartridge (SEP-PAK light, Waters Accell Plus QMA, USA) that was connected to the ASU. A mixture of CH_3CN (400 µL) containing K_{222} (22 mg) and water (400 µL) containing K_2CO_3 (7.5 mg) was used to elute [^{18}F]fluoride from the QMA cartridge into the reaction vial. Using an automated programmed synthesis sequence, the reaction vial contents were dried (110 °C; 7 min), followed by the addition of tosylate precursor (**5;** 5 mg) in anhydrous

CH_3CN (2 mL) to the reactor for labeling at 100 °C for 10 min. The mixture was then diluted with water (25 mL) and the resulting solution was pushed through a C-18 Sep-Pak cartridge. The cartridge was rinsed with an additional volume of water (10 mL) to remove unreacted fluoride and other polar impurities, and then flushed with aqueous NaOH (0.1 N; 2 mL) and kept static for 2 min to effect alkaline hydrolysis of β-Ac_2[^{18}F]FAZA which had been retained on the cartridge. Impure β-[^{18}F]FAZA **6a** was eluted from the cartridge using aqueous NaH_2PO_4 (0.5 N; pH 6-7.5) buffer solution, and purified on HPLC using a Phenomenex Luna pre-column C18/2 (50 x 10 mm, 5 μm) and Phenomenex Nucleosil C18 column (250 x 10 mm, 5 μm). EtOH:NaH_2PO_4 buffer was used as a mobile phase (8:92, v/v; flow rate 5 mL/min). Purified β-[^{18}F]FAZA **6a** and another F-18 labeled species **6b** ([^{18}F]Peak **2**) that eluted at 11.2 and 20.5 min, respectively, under these HPLC conditions were collected separately and sterile-filtered (0.22 μm Millex-GS filter, Millipore, USA). The overall synthesis time was 50 min (RCY ~18% decay corrected; radiochemical purity >98%). Purity and the retention times (quality control, QC) of radiofluorinated **6a** and **6b** were determined by co-injecting the purified radiofluorinated products with the reference compounds β-Ac_2-FAZA and β-FAZA on another HPLC system. This system used an Accel ODS reverse phase column (250 x 4.6 mm; mobile phase, 0.9% sterile saline:EtOH = 90:10 v/v, 1 mL/min) and on-line UV (220 and 320 nm) and radiation detectors.

Radiofluorination optimization and TRACERlab FX_{F-N} ASU method: The effects of temperature (60, 70 and 100 °C), nature of the base in the eluent (0.5M K_2CO_3 or 0.5M $K_2C_2O_4$ or a 1:1 mixture of K_2CO_3 and $K_2C_2O_4$), reaction time (1, 3, 5, 10, 20 and 30 min) and reagent for hydrolysis (0.05 N NaOH or 0.2 N NH_4OH) on the radiochemical yields of β-[^{18}F]FAZA, **6a** were investigated. After azeotropic drying (anhydrous CH_3CN; 2 x 100 μL) of the [^{18}F]fluoride in the reactor, the tosylate precursor (**5**, 5 mg) in anhydrous DMSO (1 mL) was added and the labeling was carried out under stirring at pre-determined temperatures and times (Figure 3). Deprotection of the labeled product was performed by adding aqueous NaOH (1 mL; 0.1 N or 0.05 N) or NH_4OH (1 mL; 0.2 N) at 30 °C for designated times, and then pH was neutralized by adding aqueous NaH_2PO_4 (0.5 mL; 0.5 N) to bring it in a range of 6-7.5. The radiolabeling yields were quantified by TLC on silica gel plates (POLYGRAM SIL G/UV_{254}, 40*80 mm, Macherey & Nagel, Düren, Germany) developed using ethyl acetate. Radioactive spots were quantitatively assessed by means of an electronic autoradiograph (InstantImager, Canberra Packard, USA). Rf values for [^{18}F]fluoride, β-[^{18}F]FAZA **6a** and β-Ac_2[^{18}F]FAZA **6** were 0.00, 0.62 and 0.77, respectively. (Table 1)

Automated synthesis process for β-[^{18}F]FAZA **6a** using the Tracerlab module was based on the optimized reaction parameters as described above, which included radiofluorination of the tosylated precursor **5** (5 mg) at 60 ºC over a period of 10 min, followed by the alkaline deacetylation of β-Ac_2[^{18}F]FAZA using 0.2N.NH_4OH solution. In brief, [^{18}F]-fluoride was eluted from the preconditioned cartridge using the eluent (15 mg K_{222} in 900 µL acetonitrile and 0.5M.K_2CO_3 in 50 µL sterile water), and azeotropically dried in the ASU reactor at 140 ºC. The reactor was then cooled down to 60 ºC, the tosylate precursor pre-dissolved in anhydrous DMSO (1 mL) dropped in, and the labeling continued for 10 min. After cooling the reaction mixture to 30 ºC, 0.2N.NH_4OH solution (1 mL) was added to materialize the deacetylation (2 min), and the impure labeled mixture was chromatographed on the reversed phase HPLC using a Supelcosil ABZ column (250 x 6 mm, 5µ) column using Ethanol (96%): 10 mM Na_2HPO_4 solution (8:92, v/v) as eluent (flow rate 4 mL/min). β-Ac_2[^{18}F]FAZA, β-[^{18}F]FAZA and **6b** ([^{18}F]-Peak **2)** eluted at 9.49, 5.48 and 7.7 min, respectively using this system (Table 1).

Table 1. Chromatographic characteristics of β-[^{18}F]FAZA, **6a**, and the major radiofluorination by-product (**6b**; [^{18}F]Peak **2**) using TracerLab FX_{F-N} ASU. The HPLC 'Peak Area' refers to the signal intensity of the respective chromatographic peak for a given purification. The retention time for the radiofluorination precursor β-Ac_2[^{18}F]FAZA is provided for reference purposes. TLC Rf values are also included.

Detector	**β-[^{18}F]FAZA (6a)**		**[^{18}F]Peak 2 (6b)**		**β-Ac_2[^{18}F]FAZA**
	HPLC Retention Time (min)[2]	Peak Area	HPLC Retention Time (min)[2]	Peak Area	HPLC Retention Time (min)[3]
Radio-activity	5.6	832732	7.7	529957	9.5
UV 320 nm	5.2	4962	7.4	2685	9.4
UV 254 nm	5.2	7247	7.4	694	9.4
TLC Rf[1]	0.62	-	0.7	-	0.77

[1]Rf on POLYGRAM SIL G/UV_{254}, developed using ethyl acetate
[2]solvent system: CH_3CN:H_2O = 3:97 v/v, 2 mL/min

β-[^{18}F]FAZA Stability Studies

Purified β-[^{18}F]FAZA, obtained as a solution in ethanol (8%) in NaH_2PO_4 buffer (92%), was stored in a sterile multi-dose vial at 22 °C. Stability and the purity of β-[^{18}F]FAZA radiopharmaceutical was determined by HPLC analysis immediately upon packaging (0 h) and then after 2.5, 4 and 8 h, using a

Phenomenex column (250 x 4.6 mm, 5 μm) and CH_3CN:H_2O (3:97, v/v; 2 mL/min) as eluent. (Figure 2)

PET imaging of A431 tumor xenografts in athymic nude mice

Animal imaging was based on detailed procedures published elsewhere [25]. BALB/c nude mice, 8–12 weeks old, were obtained from the Animal Resources Centre (Perth, Western Australia) and housed in microisolator boxes. Xenografts were established by injecting 3×10^6 exponentially growing A431 cells (American Type Culture Collection) in PBS (50 μL) into the sub-cutaneous tissue above the right forelimb of anaesthetized mice. Imaging experiments were done when tumors had reached a size of 200 mm^3. PET imaging was done using a dedicated small animal PET scanner (Mosaic, Philips, Cleveland, OH). This scanner has an effective axial field of view of 11.6 cm and measured resolution of 2.26 mm at the center of the field of view. On the basis of previous biodistribution studies conducted in A431 xenografts-bearing nude mice, PET scan acquisition was started 3 h after administration of β-[^{18}F]FAZA (25-30 MBq) given by tail vein injection. A static 15-min scan was obtained with the mouse immobilized and anaesthetized in a container into which 2% isoflurane gas was mixed in equal parts with oxygen and air, delivered at a total rate of 400 mL/min. A single bed position acquisition was sufficient to encompass the whole of the body of the mouse. Attenuation correction, either measured or estimated, was not done. Scans were acquired in a three-dimensional volume mode, and rebinned into two-dimensions using a Fourier algorithm. The data were reconstructed using the ordered subset expectation maximization technique (four iterations and eight subsets) into 1-mm transaxial slices. Institutional animal ethics committee approval was obtained for all experiments.

Results and Discussion

Chemistry. β-Ac_2AZA, **3**, the common synthon for β-FAZA **6** and its tosylate precursor **5**, was obtained either by inversion of configuration at *C2'* of azomycin riboside (AZR; **1;** [24]) or by de novo coupling of azomycin and arabinose to obtain AZA, **2**, followed by selective sequential protection of *C5'*-OH (*tert*-butyldiphenyl silylation) and *C2',C3'*-OHs (acetylation), and then desilylation at *C5'*. Although the AZR approach has the advantage of starting with commercially-available AZR, both approaches utilize classical methods.[24] DAST-based fluorination of **3** afforded β-Ac_2FAZA, **4**, but total conversion of the precursor **3** to **4** was not attained. Unreacted **3** and **4** (30% yield) were purified by column chromatography and recovered from the reaction mixture. ^{1}H- and ^{13}C-NMR spectra of **4** demonstrated typical *F-H* ($J_{F\text{-}H5''}$ = 46 Hz; $J_{F\text{-}H5'}$ = 47.5 Hz $J_{F\text{-}H4'}$ = 25.9 Hz) and *F-C* ($J_{F\text{-}C5'}$ = 174.7 Hz;

$J_{F\text{-}C4'}$ = 19.8 Hz; $J_{F\text{-}C3'}$ = 6.6 Hz) coupling constants that confirmed the incorporation of fluorine at *C5'* in **4**. ^{19}F-NMR spectrum corresponded to the *F-H* and *F-C* coupling patterns that are in accordance with previous reports [26]. Alkaline hydrolysis of this product using 2MNH_3 in methanol yielded β-FAZA **6** in 70% yield, somewhat lower that the 96% reported for deprotection of β-Ac_2IAZA [24]. ^{1}H, ^{13}C and ^{19}F-NMR spectral characterization confirmed that fluorine was not lost during the deacetylation process. Deacetylation moved the chemical shifts of the corresponding carbons (*C2'* and *C3'*) upfield in **6**, and also demonstrated a stronger fluorine interaction with *C4-C5* plane of the nitroimidazole plane ($J_{F\text{-}C5}$*NI* = 5.5 Hz). (Table 2)

Spatial orientation of fluorine on *C5'* will strongly impact the protons and carbons of the nitroimidazole moiety, depending on the plane facing fluorine. Interestingly, nitroimidazole-*C5* in both **4** and **6** demonstrated a clear fluorine-carbon electronic interaction (β-Ac_2FAZA, $J_{F\text{-}C5}$*NI* = 3.3 Hz; β-FAZA, $J_{F\text{-}C5}$*NI* = 5.5 Hz); no such interactions are exhibited by α-FAZA carbons. [26] Further, imidazole (*Im*)-*H5* in β-FAZA **6**, appears to be influenced by strong *F-H* inductive bonding and demonstrates a downfield chemical shift (δ 7.57) in comparison to *Im-H-5* proton (δ 7.14) in α-FAZA. This reveals that spatial orientation of fluorine in β-FAZA is in the same plane as imidazole ring, and imidazole *H5-H4* plane is *facing* fluorine while the nitro group is protruding on the opposite side. *F-Im-C5* electronic interactions in β-FAZA ($J_{F\text{-}C5\text{-}Im}$ = 5.5 Hz) and its acetylated derivative **4** further support this hypothesis. In case of α-FAZA, not only are *F-Im-C4-C5* interactions absent, [26] the formation of a cyclic product due to the reaction between *C2'*-OH and the *Im-C2*-NO_2 group during the synthesis of α-AZA is also observed.[27] All of these findings establish that the orientation of fluorine and the *Im-H4-H5* plane in α-FAZA is *away* from each other and *below* the plane (α-configuration). *Im-H4* is further away from fluorine, therefore remains unaffected in both α- and β-FAZAs.

Similar orientations were earlier reported for the iodo analogue, 1-β-D-(5-iodo-5-deoxyarabinofuranosyl)-2-nitroimidazole (β-IAZA), based on NOE and atomic distance estimates obtained from the optimized structure [24]. A comparison of the chemical shifts of the protons and the carbons in β-AZA, β-FAZA, β-Ac_2FAZA, α-FAZA and α-Ac_2FAZA, and the *J* values for the nuclei interacting with fluorine are provided to support our findings (Table 2).

Table 2. Proton NMR Coupling constants for β-AZA, β-FAZA, β-Ac_2FAZA, α-FAZA and α-Ac_2FAZA

Compds		**δ ^{1}H ppm ($J_{F\text{-}H}$ in Hz)**	**δ ^{13}C ppm ($J_{F\text{-}C}$ in Hz)**	**δ ^{19}F[a]**

.														ppm
	H5''	***H5'***	***H4'***	***H3'***	**H2'**	***Im-H5***	***Im-H4***	***C5'***	***C4'***	***C3'***	***Im-C2***	***Im-C5***	***Im-C4***	
β-AZA[24]	3.89	3.81	3.95	4.04	4.42	7.97 (1.2)	7.13 (1.2)	61.78	85.90	75.79	145.82	125.16	127.87	-
β-FAZA	4.69 (48.8)	4.76 (48.8)	4.07 (24.4)	4.00	4.47 (1.2)	7.57	7.15	82.43 (171.4)	83.48 (18.7)	74.55 (6.6)	145.31	124.19 (5.5)	128.07	-65.37
α-FAZA[26]	4.20 (57)	4.20 (57)	4.60 (br)	4.50 (6.0)	4.66 (br)	7.14	7.68	83.63 (169.7)	89.04 (20.6)	77.21 (4.7)	NR	125.22	128.25	-71.17
β-Ac_2-FAZA	4.71 (46)	4.76 (47.5)	4.27 (25.9)	5.21	5.73 (ND)	7.57	7.19	80.82 (174.7)	81.54 (19.8)	74.86 (6.6)	145.31	122.98 (3.3)	128.25	-69.37
α-Ac_2-FAZA[26]	4.65 (47.5)	4.65 (47.5)	4.64 (19.5)	5.15	5.23 (br)	7.20	7.37	81.64 (175.7)	85.95 (19.2)	75.97 (6.2)	144.80	121.89	128.49	

[a]Fluorine chemical shifts are reported with respect to $CFCl_3$; NR = not reported, br = broad signal

Compound **3**, also a synthon to the precursor for β-[^{18}F]FAZA, was tosylated to afford 5'-*O*-tosyl-Ac_2-β-AZA, **5**, in 70% yield; classical tosylation conditions were used for this synthesis.

Radiochemistry. Extensive studies were performed to optimize the radiofluorination yields of β-[^{18}F]FAZA. Automated syntheses processes using Coincidence and GE-TRACERlab FX_{F-N} syntheses units were also developed to validate the clinical manufacturing process, and the stability of purified β-[^{18}F]FAZA radiopharmaceutical was determined to establish the radiochemical and chemical integrities for its future clinical use.

The effects of radiolabeling temperature, the base used for ^{18}F-complex formation with K_{222}, and the base used for removing the protective acetyl groups from β-Ac_2[^{18}F]FAZA on radiofluorination yields of β-[^{18}F]FAZA were investigated. DMSO, the solvent of choice for FAZA labeling, was used for radiosynthesis. Radiofluorination was explored at 60, 70 and 100 ºC. K_2CO_3 (0.5M; 50 µL) and K_{222} (15 mg) were used for generating [^{18}F]fluoride-K_{222} complex in these reactions (Fig. 3A-C). The study demonstrated that, at 100 ºC β-[^{18}F]FAZA formation was surpassed by the formation of a secondary radiofluorinated product (Table 1; **6b**; [^{18}F]Peak **2**) right from the start of synthesis. RCYs of β-[^{18}F]FAZA reached nearly 37% in ~3 min, but then deteriorated sharply (~16% at 10 min and ~6% at 20 min); [^{18}F]Peak **2** formation rose to ~48% in 20 min (Fig. 3B). At 70 ºC, the reaction kinetics for β-[^{18}F]FAZA formation were more controlled (37% β-[^{18}F]FAZA and 8% [^{18}F]Peak **2** formation after 5 min), but at longer reaction times β-[^{18}F]FAZA started to deteriorate (RCYs for β-[^{18}F]FAZA, 33%, and for [^{18}F]Peak **2**, 17% 10 min post-radiofluorination) (Fig 3A). Reducing the labeling temperature to 60 ºC further slowed down the kinetics for [^{18}F]Peak **2** formation (3% after 5 min and 8% after 10 min), and also improved β-[^{18}F]FAZA formation (38% after 5 min and 44% after 10 min; Fig 3C).

The chemical identity of [^{18}F]Peak **2** could not be determined, but the presence of a corresponding uv absorption peak at 320 nm implies that it is an azomycin derivative. The radioactivity:uv peak area ratios for β-[^{18}F]FAZA and [^{18}F]Peak **2** (168 and 197, respectively) and relatively longer retention time for [^{18}F]Peak **2** in comparison to β-[^{18}F]FAZA imply that the chemical structure of [^{18}F]Peak **2** is closely related to β-[^{18}F]FAZA. In other words, [^{18}F]Peak **2** is neither a nitro-elimination product nor a nucleoside decomposition product. [^{18}F]Peak **2** is also not a *C5*' elimination product since it would not be radioactive. It is possible that Peak-**2** represents the corresponding *C5'*-F, *C2'-C3'* oxiranyl azomycin nucleoside. The formation of 2',3'-oxiranyl-α-FAZA during the 'single step' synthesis of α-FAZA has been confirmed [27] and it is postulated that it is a side product of thermal deacetylation at *C2'* and *C3'* under basic radiofluorination (K_2CO_3) conditions. Further work is required to completely characterize the chemical structure of this side-product.

Using a mixture of potassium oxalate (0.5 M) and potassium carbonate solution (0.5M) (25 µL each) as the base for [^{18}F]fluoride-K_{222} complex formation provided the best reaction profile for β-[^{18}F]FAZA (~51% RCY in 10 min) and minimized the secondary reactions (~5%; Fig 3D). This indicates that the hardness of the base (K_2CO_3) plays a major role in directing the formation of the alternate radiofluorinated species. Use of only potassium oxalate (no potassium carbonate) in the eluent led to very poor radiofluorination yield (<5%).

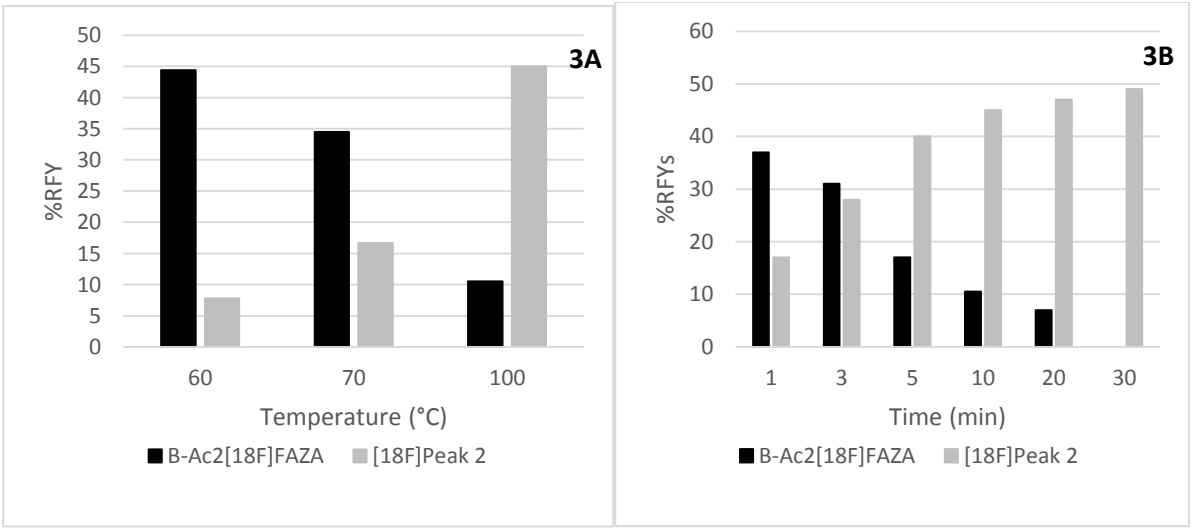

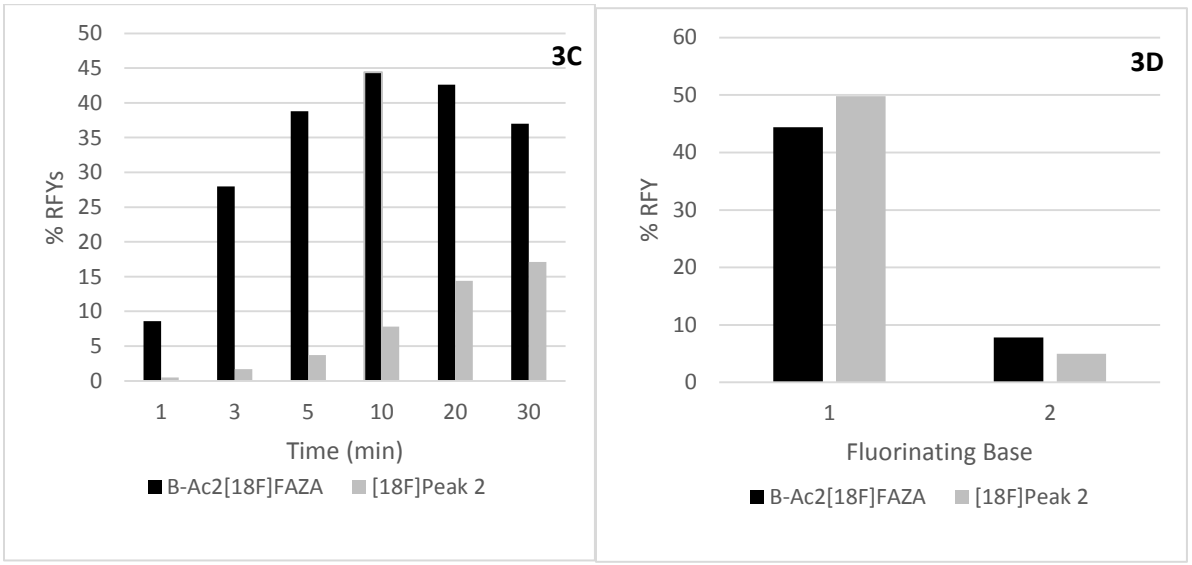

Figure 3. A comparison of the radiofluorination yields (RFYs) of β-Ac_2[^{18}F]FAZA and the secondary labeled product at: **3A)** 60, 70 and 100 °C at 10 min post-radiofluorination using K_{222} (15 mg) + 0.5M K_2CO_3 (50 µL) as eluent in acetonitrile: water (50 µL; 1:1 v/v); **3B)** 100 °C; indicating that the formation of β-Ac_2FAZA rises to >30% in 3 min, but is also accompanied by a secondary product, [^{18}F]Peak **2**; **3C)** 60 °C; the formation of β-Ac_2[^{18}F]FAZA progresses smoothly and β-[^{18}F]FAZA is recovered in ~48% RFY with nominal [^{18}F]Peak **2** formation (8%) in 10 min.; **3D)** 60 °C and 10 min labeling time using K_{222} (15 mg) and K_2CO_3 (0.5M, 50 µL) as eluent, and K_{222} (15 mg) and K_2CO_3 (0.5M, 25 µL) + potassium oxalate (0.5M, 25 µL) as eluent; the RFY for β-[^{18}F]FAZA further improved **(3D-1)** and the side product formation was minimal **(3D-2)** when a mixture of K_2CO_3 and $K_2C_2O_4$ was used as the base in the eluent.

Automated Synthesis. The synthesis of β-[^{18}F]FAZA was validated on two ASUs, Coincidence, and GE TRACERlab FX_{F-N}. The basic difference between the two ASU methods was that the Coincidence ASU used anhydrous CH_3CN as a reaction solvent and a disposable synthesis cassette, whereas the TRACERlab ASU used anhydrous DMSO as the labeling solvent and an integrated synthesis system for the radiofluorination procedure. Hydrolysis of the protective groups was performed on a solid phase Sep-Pak™ cartridge in case of the Coincidence ASU, while all the steps of synthesis were undertaken in the reaction vessel in the TRACERlab ASU. HPLC purification of β-[^{18}F]FAZA was required in both cases.

Once [^{18}F]fluoride was isolated, complexed with K_{222}/K_2CO_3 and azeotropically dried, the radiosynthesis procedures diverged to exploit the characteristics of the ASUs used. Radiofluorination process involved the nucleophilic substitution of β-Ac_2TsAZA with the $^{18}F/K_{222}$ complex, followed by

deacetylation via alkaline hydrolysis to afford β-[^{18}F]FAZA, **6a**. As described above, a HPLC-based purification (both Coincidence and GE TRACERlab) of impure product composed in citrate buffer, afforded pure β-[^{18}F]FAZA.

Stability Studies. The purified product was subjected to the HPLC analysis at 1, 2.5, 4 and 8 h post-purification to evaluate its potential use in the clinic and storage over extended time period. The studies indicated that the integrity of β-[^{18}F]FAZA radiopharmaceutical, once purified, was stable over a period of eight hours when stored in aqueous ethanol at 0-5 ˚C. (Fig. 4)

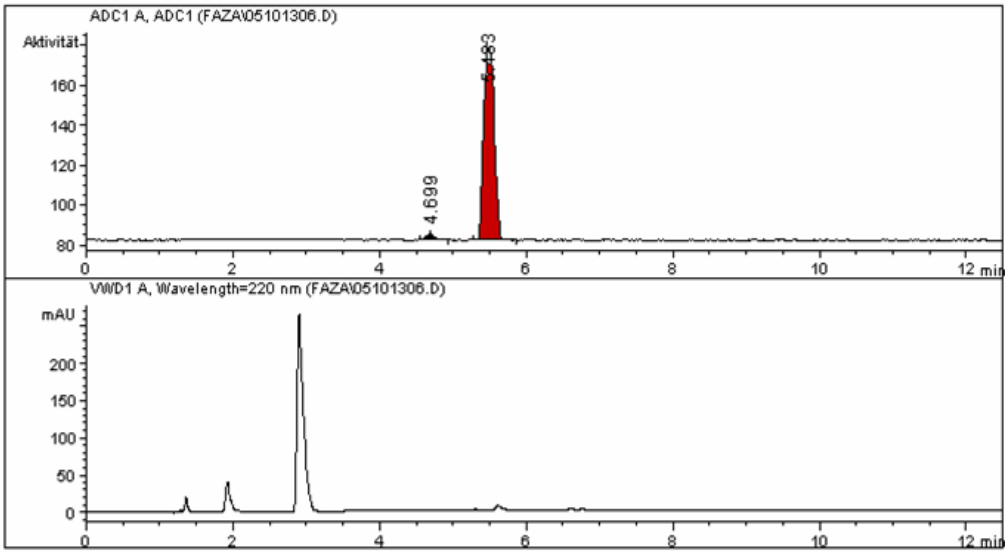

Figure 4. HPLC chromatogram of an ethanolic solution containing β-[^{18}F]FAZA (larger filled peak; upper chromatogram) and a small radiochemical impurity (small, left peak; upper chromatogram) at 8 h. Peaks representing uv-detectable chemical impurities at 220 nm are visible in the lower scan.

PET imaging

β-[^{18}F]FAZA injected into mice implanted with A431 tumors provided classical images of biodistribution, including uptake by tumor and liver, and distribution within the lower gastro-intestinal tract (Fig. 5). Autoradiographic image slices revealed accumulation primarily in selected regions on the periphery of the tumor, but also local regions within the tumor volume, consistent with regions of hypoxia and necrosis in a large tumor. All β-[^{18}F]FAZA images were qualitatively similar to [^{18}F]FAZA images (not shown) in the same murine tumor model. Additional quantitative studies, including head-to-head comparisons with [^{18}F]FAZA, are required to determine whether or not the

conformation at *C1*, the anomeric centre, has any impact on biodistribution, excretion or metabolism that might alter hypoxia-specific uptake or sensitivity.

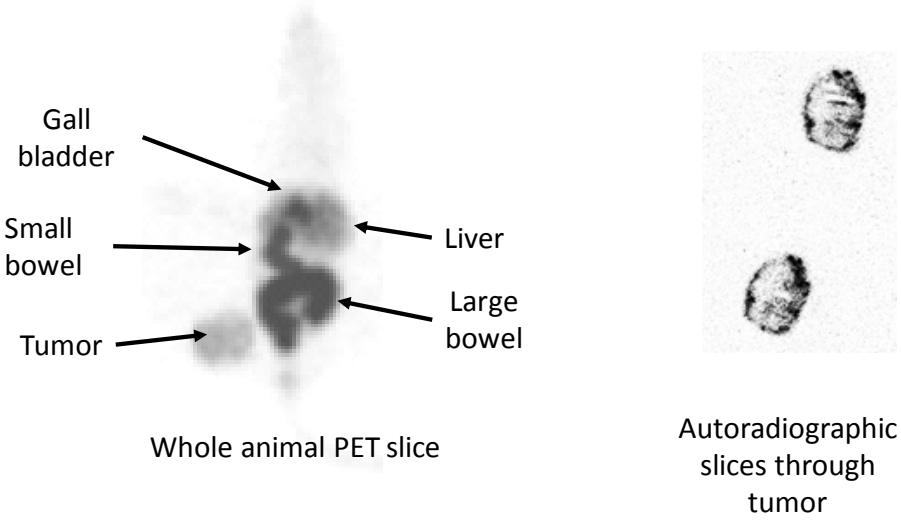

Figure 5. β-[^{18}F]FAZA imaging in a Swiss Nude Mouse bearing an implanted A431 tumor. The whole animal image (left) shows uptake by tumor and the hepato-biliary system. Heterogenous distribution of hypoxic regions is seen in the tumor autoradiographs (right) that show an irregular uptake pattern of β-[^{18}F]FAZA on the tumor periphery, and throughout the tumor. The injection dose was 30 MBq administered via the tail vein; the image was acquired 60 min post- injection.

Summary

β-FAZA, was obtained in good yield (21%) from standard azomycin nucleoside precursors. Radiofluorination of the tosylate precursor afforded β-[^{18}F]FAZA in up to ~51% RCY. Higher radiolabeling yields were obtained in the presence of a K_2CO_3 / $K_2C_2O_4$ mixture in comparison to $K_2C_2O_4$ or K_2CO_3 alone. The formation of a radiolabelled side product ([^{18}F]Peak **2** (**6b**) was shown to be dependent on both labeling and deprotection conditions. The best yields (~18% RCY) of β-[^{18}F]FAZA from β-Ac_2[^{18}F]FAZA were obtained by deprotecting the labeled product using a mild base, whereas deprotection with NaOH led to almost total conversion to [^{18}F]Peak **2**. For radiofluorination of the tosylated precursor, the best product to [^{18}F]Peak **2** ratios were obtained at low temperatures (60 °C) with short (10 min) reaction times. β-[^{18}F]FAZA was radiochemically stable in

8% EtOH/phosphate buffer solution at 22 ºC for up to 8 h. Initial qualitative PET images in A431 tumor bearing mice showed uptake patterns consistent with hypoxia-specific uptake in this model.

Acknowledgements

This research was supported by grants from the Alberta Cancer Board, and by operating funds from the Peter MacCallum Cancer Center in Melbourne and the University of Tübingen in Germany.

REFERENCES

[1] Gray, L.H.; Conger, A.D.; Ebert, M.; Hornsey, S.; Scott, O.C. The concentration of oxygen dissolved in tissues at the time of irradiation as a factor in radiotherapy. *Br. J. Radiol*., **1953**, 26, 638-648.

[2] Tomlinson, R.H.; Gray, L.H. The histological structure of some human lung cancers and the possible implications for radiotherapy. *Br. J. Cancer*, **1955**, 9, 539-549.

[3] Wilson, W.R.; Hay, M.P. Targeting hypoxia in cancer therapy. *Nature Rev. Cancer*., **2011**, 11, 393-410.

[4] McDonald, P.C.; Chafe, S.C.; Dedhar, S. Overcoming hypoxia-mediated tumor progression: combinatorial approaches targeting pH regulation, angiogenesis and immune dysfunction. *Front. Cell Dev. Biol*., **2016**, http://dx.doi.org/10.3389/fcell.2016.00027.

[5] Walsh, J.C.; Lebedev, A.; Aten, E.; Madsen, K.; Marciano, L.; Kolb, H.C. The clinical importance of assessing tumor hypoxia: relationship of tumor hypoxia to prognosis and therapeutic opportunities. *Antioxid. Redox Signal*., **2014**, 21, 1516–1554.

[6] Vaupel, P.; Mayer, A. Hypoxia in cancer: significance and impact on clinical outcome. *Cancer Metastasis Rev*., **2007**, 26, 225-239.

[7] Harada, H. How can we overcome tumor hypoxia in radiation Therapy? *J. Radiat. Res*., **2011**, 52, 545-556.

[8] Biaglow, J.E.; Varnes, M.E.; Roizen-Towle, L.; Clark, E.P.; Epp, E.R.; Astor, M.B.; Hall, E.J. Biochemistry of reduction of nitro heterocycles. *Biochem. Pharmacol*., **1986**, 35, 77-90.

[9] Adams, G.E.; Flockhart, I.R.; Smithen, C.E., Stratford, I.J.; Wardman, P.; Watts, M.E. Electron-affinic sensitization VII. A correlation between structures, one-electron reduction potentials, and efficiencies of nitroimidazoles as hypoxic cell radiosensitizers. *Radiat Res*., **1976**, 67, 9-20.

[10] Graves, E.E.; Hicks, R.J.; Binns, D.; Bressel, M.; Le, Q-T.; Peters, L.; Young, R.J.; Rischin, D. Quantitative and qualitative analysis of [^{18}F]FDG and [^{18}F]FAZA positron emission tomography of head and neck cancers and associations with HPV status and treatment outcome. *Eur. J. Med. Mol. Imaging.*, **2016**, 43, 617-625.

[11] Kumar, P.; Bacchu, V.; Wiebe, L.I. The chemistry and radiochemistry of hypoxia-specific radiohalogenated nitroaromatic imaging probes. *Sem. Nucl. Med*., **2015**, 45, 122-135.

[12] Peters, S.G.J.A.; Zegers, C.M.L.; Yaromina, A.; van Elmpt, W.; Dubois, I.; Lambin, P. Current pre-clinical and clinical applications of hypoxia PET imaging using 2-nitroimidazoles. *Q. J. Nucl. Med. Mol. Imaging.*, **2015**, 59, 39-57.

[13] Emami, S.; Kumar, P.; Yang, J.; Kresolic, Z.; Paproski, R.; Cass, C.; McEwan, A.J.; Wiebe, L.I. Synthesis, transportability and hypoxiaselective binding of 1-β-D-(5-deoxy-5-fluororibofuranosyl)-2-nitroimidazole (β-5-FAZR), a configurational isomer of the clinical hypoxia marker, FAZA. *J. Pharm. Pharm. Sci*., **2007**, 10, 237-45.

[14] Malik, N.; Xian, L.X.; Loffler, D.; Shen, B.; Solbach, C.; Reischl, G.; Voelter, W.; Machulla. H-J. Synthesis of O-[2-[^{18}F]fluoro-3-(2-nitro-1H-imidazole-1-yl)propyl]tyrosine ([^{18}F]FNT]) as a new class of tracer for imaging hypoxia. *J. Radioanalyt. Nucl. Chem*., **2012**, 292, 1025-1033.

[15] Sorger, D.; Patt, M.; Kumar, P.; Wiebe, L.I.; Barthel, H.; Seese, A.; Dannenberg, C.; Tannapfe, A.; Kluge, R.; Sabri, O. Comparison of [^{18}F]fluoroazomycinarabinoside ([^{18}F]FAZA) and [^{18}F]fluoromisonidazole ([^{18}F]FMISO) as hypoxia tracers: quantitative cell culture studies and PET imaging of experimental rat tumors. *Nucl. Med. Biol.*, **2003**, 30, 317-326.

[16] Wuest, M.; Kumar, P.; Wang, M.; Yang, J.; Jans, H.S.; Wiebe, L.I. In vitro and in vivo evaluation of [^{18}F]F-GAZ, a novel oxygen-mimetic azomycin-glucose conjugate, for imaging hypoxic tumor. *Cancer Biother Radiopharm*., **2012**, 27, 473-480.

[17] Wanek, T.; Kreis ,K.; Križková, P.; Schweifer, A.; Denk, C.; Stanek, J.; Mairinger, S.; Filip, T.; Sauberer, M.; Edelhofer, P.; Traxl, A.; Muchitsch, V.E.; Mereiter, K.; Hammerschmidt, F.; Cass, C.E.; Damaraju, V.L.; Langer, O.; Kuntner, C. Synthesis and preclinical characterization of 1-(6'-deoxy-6'-[^{18}F]fluoro-β-d-allofuranosyl)-2-nitroimidazole (β-6'-[^{18}F]FAZAL) as a positron emission tomography radiotracer to assess tumor hypoxia. *Bioorg. Med. Chem*., **2016**, 24, 5326-5339.

[18] Alauddin, M.M. Positron emission tomography (PET) imaging with ^{18}F-based radiotracers. *Am. J. Nucl. Med. Mol. Imaging*., **2012**, 2, 55-76.

[19] Wu, J. Review of recent advances in nucleophilic C–F bond-forming reactions at sp3 centers. *Tetrahedron Lett*., **2014**, 55, 4289-4294.

[20] Furuya, T.; Kamlet, A.S.; Ritter, T. Catalysis for fluorination and trifluoromethylation. *Nature.*, **2011**, 473, 470-477.

[21] Farah, S.F.; McClelland, R.A. Preparation and reactions of bromo-2-nitro- and bromo-2-aminoimidazoles. *Can. J. Chem*., **1993**, 71, 427-432.

[22] Wiebe, L.I.; Sun, W.; Kumar, P. unpublished.

[23] Zhang, H.; Cantorias, M.V.; Pillarsetty, N.; Burnazi, E.M.; Cai, S.; Lewis, J.S. An improved strategy for the synthesis of [^{18}F]-labeled arabinofuranosyl nucleosides. *Nucl. Med. Biol*., **2012**, 39, 1182-1188.

[24] Kumar, P.; Ohkura , K.; Beiki, D.; Wiebe, L.I.; Seki, K-I. Synthesis of 1-β-D-(5-deoxy-5-iodoarabinofuranosyl)-2-nitro-imidazole (β-IAZA): a novel marker of tissue hypoxia. *Chem. Pharm. Bull.*, **2003**, 51, 399-403.

[25] Solomon, B.; Binns, D.; Roselt, P.; Wiebe, L.I.; McArthur, G.A.; Cullinane, C.; Hicks, R.J. Modulation of intratumoral hypoxia by the epidermal growth factor receptor inhibitor gefitinib detected using small animal PET imaging. *Mol. Cancer Ther*., **2005**, 4, 1417-1422.

[26] Kumar, P.; Stypinski, D.; Xia, H.; McEwan, A.J.B.; Machulla, H-J.; Wiebe, L.I. Fluoroazomycin arabinoside (FAZA): synthesis, ^{3}H and ^{3}H-labelling and preliminary biological evaluation of a novel 2-nitroimidazole marker of tissue hypoxia. *J. Labelled Compd. Radiopharm*., **1999**, 42, 3-16.

[27] Kumar, P.; Emami, S.; McEwan, A.J.B.; Wiebe, L.I. Development of an economical, single step synthesis of FAZA, a clinical hypoxia marker, and potential synthons to prepare its positional analogs. *Lett. Drug Design Discovery.*, **2009**, 6, 82-85.